Biophysical Chemistry 11 (1980) 39–47
© North-Holland Publishing Company

JAHN–TELLER EFFECT IN BIOMOLECULES

M. BACCI
Istituto di Ricerca sulle Onde Elettromagnetiche of C.N.R.,
Firenze, Italy

Received 30 January 1979
Revised manuscript received 10 July 1979

The role played by the Jahn-Teller effect for a correct interpretation of the spectroscopic and structural data of some biological systems is stressed and a short review of the investigations so far performed is presented. Afterwards, on the basis of the angular overlap model, several expressions are given for the coupling constants of the transition metal ions, which mainly occur in biomolecules (Fe, Co, Cu, Mo) in order to have an approximate evaluation of the Jahn-Teller effect magnitude. The above expressions are then applied to obtain the vibronic coupling constants of the deoxygenated hemoglobin and myoglobin. The results obtained are compared with the predictions previously made by the author on these systems.

1. Introduction

Metalloproteins play an essential role in many biological processes [1]. They act as metal storage and transport proteins, oxygen carriers and enzymes, whose activity mainly depends upon a locally energised metal-protein conformation [2]; hence it is important to know the stereochemistry and electronic structure of the chromophores containing the metal ion. Naturally occurring metalloproteins are often characterized by unusual geometries, due to the constraints imposed by the specific secondary and tertiary structure of the protein. However, apart from the cause of the distortion, the prosthetic group can be considered alike a common coordination compound with the same geometry.

Many attempts have been made to interpret the experimental data on the basis of the crystal field or molecular orbital theory and a particular attention was paid to hemoproteins [3]; each theoretical approach provides certain insights, although a complete interpretation of the phenomenology can be hardly reached.

Another approach, particularly suitably for highly distorted structures, is constituted by the angular overlap model (AOM) [4–7], which has been barely exploited for biomolecules as yet [8]. The AOM represents a simplification of the LCAO-MO theory in the Wolfsberg-Helmholz approximation [9] and has the advantage of a very limited number of parameters, which possess some degree of physical interpretability and are transferable from one chromophore MX_q to another MX_p of different symmetry, provided that all the M-X distances are the same.

The Jahn-Teller effect (JTE) is based on a theorem first described by Jahn and Teller in 1937 [10] and affirms that, if an electronic degenerate level exists in a non-linear molecule, the nuclei displace themselves in order to destroy the symmetry of their configuration and to remove the electronic degeneracy.

Many years elapsed before the importance of the JTE in the interpretation of spectroscopic and structural properties of molecules and crystals was recognized and it was only in the fifties and sixties that the JTE was developed and demonstrated to be effective in a large amount of physical systems [11]. Indeed one can say that the JTE cannot be ruled out *a priori*, but only when it is proved to be absent or negligible; therefore it is important to know, at least approximately, the magnitude of the effect.

The first attempt of calculating the Jahn-Teller coupling constants was made by Van Vleck in 1939 [12] on the basis of the crystal field theory and successively this method or the ligand field method [13,14] were followed, but the resulting expressions, apart from the consistency of the calculated values with the experimental data, are rather inconvenient to handle owing to the large number of parameters.

Very recently the author of the present paper has introduced a new parameterization method, based on the AOM, which allows qualitative previsions on different Jahn-Teller systems and a semi-quantitative evaluation of the coupling constants [15].

At this point I would like to remark that to talk about the JTE in biomolecules could appear contradictory; in fact the JTE is characteristic of highly symmetrical systems, where electronic degeneracy is possible, whereas, as previously said, low symmetries are typical for biomolecules. However, the JTE may represent one of the causes of the chromophore distortion, taking into account that low-symmetry perturbations can be vibronically amplified [16]. Moreover it has to be remarked that a complete degeneracy is not necessary, because it is sufficient that electronic levels are energetically close enough in order that the system is subject to JTE (pseudo-JTE). From a more quantitative point of view the following relationship should be verified [16]:

$$\Delta < a^2/K, \tag{1}$$

where 2Δ is the energy separation between the levels, a is the vibronic coupling constant and K the force constant.

In the following sections, after a short survey on the different biomolecules whose properties have been interpreted so far by the JTE, general expressions are given for the Jahn-Teller coupling constants of the transition metal ions commonly involved in metalloproteins, in various symmetries. The results are then discussed and applied to the deoxygenated hemoglobin and myoglobin (DeoxyHb and DeoxyMb, respectively).

2. Historical survey

To our knowledge the first application of the JTE to a biological molecule is due to Kamimura and Mizuashi [17,18], who attempted to explain the large anisotropy of g factors of the low-spin ferrihemoglobin azide ($g_x = 1.72; g_y = 2.22; g_z = 2.80$). They considered the combined action of the rhombic crystal field produced by the azide ion and the axial imidazole and the dynamical Jahn-Teller interaction between the electronic ground state ^2E (C_{4v} symmetry) and the stretching in-the-plane β_{1g} (henceforth we use roman letters for representations of electronic states and the corresponding greek letters for vibrational modes [19]). A good agreement with experimental data was obtained for a rhombic crystal field component of 220 cm^{-1} and a ratio $S = E_{JT}/\hbar\omega$ of ~0.64, where E_{JT} is the Jahn-Teller stabilization energy and $\hbar\omega$ the vibrational quantum.

In 1972 Weissbluth [3,20,21] gave an interpretation of the deoxygenation mechanism in oxyhemoglobin based on the JTE. It was postulated that the high spin state $^5T_{2g}$ (O_h symmetry) could be reached by thermal excitation from the low-spin ground state $^1A_{1g}$. Once this occurs, the system is subject to JTE and the most likely distortion, owing to local geometrical constraints, is along the Fe-O_2 bond, thus favouring the detachment of the oxygen molecule.

This conjecture was successively criticized on symmetry grounds because the symmetry of the chromophore is not strictly octahedral, but C_{4v}, at most, and in this point group the stretching Fe-O_2 is not Jahn-Teller active [22]. Apart from this criticism, however the interesting idea remains that the JTE may provide a local distortion, which acts as a trigger for successive conformational changes; such a triggering mechanism might be effective in other systems and could also elucidate the early stages of enzymatic activity [21].

Chan et al. in 1971 and successively Gouterman in 1973 [23] stressed the important role that could be played by the JTE in the excited triplet states of metallo-porphyrinic systems. Further Canters et al. [24,25] were able to give a proper understanding for Zeeman and MCD experiments on some metallo-porphines, by considering the vibronic coupling in the first excited singlet state ^1E_u (D_{4h} symmetry); they found for Zn-porphin a Jahn-Teller active mode at 180 cm^{-1} with a stabilization energy in the range 40–50 cm^{-1}. Another evidence of the influence of the JTE in the excited states of metallo-porphyrins arises from resonance Raman spectra of Ni-etioporphyrin and Cr-tetraphenylporphyrin chloride; in fact the comparison of the computed and observed excitation profiles shows the presence of a weak Jahn-Teller distortion in the excited Q_1 state [26].

Very recently the magnetic susceptibility and

Mössbauer data for DeoxyHb and DeoxyMb have been fitted in a C_{4v} symmetry for the chromophore FeN_5 by introducing a dynamical JTE acting on the low-lying levels [19]; in this way it is possible to overcome some inconsistencies which arise if large rhombic components are invoked to explain the magnetic and Mössbauer experimental data [27–31]. In fact X-ray structural data indicate a nearly square-pyramidal stereochemistry for the FeN_5 chromophore [32,33] and, in addition, EPR measurements show that the rhombic component is absent or negligible in very similar systems, as high spin ferric hemoglobin and myoglobin or deoxycobaltohemoglobin and deoxycobaltomyoglobin [3,34].

At last the introduction of vibronic coupling gives also a plausible interpretation [35] for the difference in magnetic moment in phosphate-free ($\mu_{\mathrm{eff}} \sim 4.90$ μ_B) and phosphate-bound ($\mu_{\mathrm{eff}} \sim 5.30$–$5.45$ μ_B) DeoxyHb [36]. In fact it was demonstrated [35] that an increase of the magnetic moment μ_{eff} corresponds to a decrease of the ratio S, previously defined. Therefore, it was suggested that the phosphate binds the globin not too far from the FeN_5 chromophore so as to hinder some vibrational modes, in particular the Jahn-Teller active β_1 mode. The mean-square amplitude δ of a normal coordinate in the harmonic approximation is given by [37]:

$$\delta = (h/8\pi^2 c\omega)\coth(hc\omega/2kT), \tag{2}$$

where ω is the vibrational frequency in cm^{-1} and the other symbols have their usual significance. A constraint on the vibrational amplitude leads to an increase of the corresponding frequency by which the value of S decreases and, consequently, the magnetic moment increases.

3. Theoretical approach

Here only a general outline of the theory will be given in order to clarify how the expressions of table 1 for different compounds are obtained, while a more complete treatment can be found elsewhere [15,38].

If the electronic potential is expanded in a series of small displacements from the undistorted configuration:

$$\begin{aligned} V = V_0 &+ \sum_{\Gamma\gamma}\left(\frac{\partial V}{\partial S^{\Gamma}_{\gamma}}\right)_0 S^{\Gamma}_{\gamma} \\ &+ \tfrac{1}{2}\sum_{\Gamma'\gamma',\Gamma''\gamma''}\left(\frac{\partial^2 V}{\partial S^{\Gamma'}_{\gamma'}\partial S^{\Gamma''}_{\gamma''}}\right)_0 S^{\Gamma'}_{\gamma'} S^{\Gamma''}_{\gamma''} + \dots \end{aligned} \tag{3}$$

where S^{Γ}_{γ} is a symmetry coordinate, corresponding to the component γ of the representation Γ, it can be demonstrated that the symmetric nuclear configuration is stable only when all the matrix elements of the linear terms

$$c = \langle\phi_i|\partial V/\partial S^{\Gamma}_{\gamma}|\phi_j\rangle \begin{cases} i = j \text{ Jahn-Teller effect} \\ i \neq j \text{ pseudo-Jahn-Teller effect} \end{cases} \tag{4}$$

are zero. The JTE is present when, for some displacements S^{Γ}_{γ} (Jahn-Teller active modes) the integral (4) does not vanish. If ϕ_i transforms as a component of the representation Γ_i, it follows from symmetry that vibrational modes may be Jahn-Teller active if the irreducible representation Γ of the coordinate S^{Γ}_{γ} is contained in the symmetric square $[\Gamma_i]^2$ [10,11].

To evaluate the magnitude of the JTE it is necessary to compute the matrix element (4). The main problem is to obtain the derivative of the potential $(\partial V/\partial S^{\Gamma}_{\gamma})$, which can be expressed in a convenient way by means of the AOM.

The AOM assumes that the energy change e_λ of a given metal orbital, due to the interaction with a ligand orbital, is

$$e_\lambda = K_\lambda S^2_\lambda F^2_{\lambda\omega}, \tag{5}$$

where λ indicates the bonding symmetry (σ, π, δ) and ω specifies the particular orbital (for π and δ bonds); S_λ is the diatomic overlap integral; $F_{\lambda\omega}$, the angular overlap factor, is a fraction of the maximum overlap integral and can be obtained from the tables of refs. [5] and [6] for a given geometry. K_λ is a proportionality constant, which is related to the energies of the metal and ligand orbitals and, in the Wolfsberg-Helmholz approximation [5,6] is given by:

$$K_\lambda \approx H^2_X/(H_M - H_X), \tag{6}$$

with H_X and H_M the energies of the ligand and metal orbitals, respectively; however, K_λ can be also considered a parameter deducible from the experimental data [15,38].

Furthermore the AOM assumes the effects of several ligands on the central metal orbital to be additive so that the general expression for the ligand field matrix element is:

$$\langle\phi_i|V|\phi_j\rangle = \sum_{\lambda\omega}\sum_{n}^{N} e_{\lambda n}\, F_{\lambda\omega}(\phi_i, X_n)\, F_{\lambda\omega}(\phi_j, X_n)\,, \quad (7)$$

where N is the coordination number.

As the symmetry coordinates S^{Γ}_{γ} can be expressed as a function of the polar coordinates θ, ϕ and the metal-ligand bond length R, the eq. (4) is rearranged, by using eq. (7), as follows:

$$c = \sum_{\lambda\omega}\sum_{n}^{N} \left\{\frac{\partial}{\partial r_n}\left[e_{\lambda n}\, F_{\lambda\omega}(\phi_i, X_n)\, F_{\lambda\omega}(\phi_j, X_n)\right]\right\} \frac{\partial r_n}{\partial S^{\Gamma}_{\gamma}}\,, \quad (8)$$

where r_n stands for the generic coordinate R_n, θ_n, ϕ_n.

Since $(\partial V/\partial S^{\Gamma}_{\gamma})$ is a one-electron operator it is a simple matter to calculate the JT constants for any configuration of a general d^n ion starting from eq. (8) [38] and using table 3 of ref. [6] to compute the F-factors. In table 1 the results for d^1, d^5, d^6, d^7 and d^9 configurations in different symmetries are reported; such results are quite general, but we have indicated in the second column of the table the metal ions, which commonly occur in metalloproteins.

4. Discussion

Since e_σ is larger than e_π (and often, but not always, a similar behaviour is true for their derivatives), a larger JTE is expected, when the coupling constant depends on e_σ (or $\partial e_\sigma/\partial R$), so that by an inspection of table 1 qualitative previsions appear particularly simple.

First of all we note the essential role played by the angle θ between the main symmetry axis and the equatorial bond M-X. Indeed the expressions for the C_{4v} and C_{3v} point groups reduce to the ones for the higher D_{4h} (or O_h) and D_{3h} symmetry, respectively, when $\theta = 90°$; in this latter case many coupling constants vanish or are strongly reduced and so it follows that the JTE is more effective in the lower symmetries. On the other hand, in a given point group, there are some values of θ, for which the coupling constants reach a maximum value; the importance of this aspect in the interpretation of the stereochemistry of DeoxyHb and DeoxyMb will be discussed later.

Let us consider now the JTE implications on the stereochemistry of blue copper proteins such as plastocyanin and azurin. These proteins function as electron-carriers in which the copper ion oscillates between Cu(II) and Cu(I) [39]; the typical coordination geometry for Cu(I) is tetrahedral, while the most favourable one for Cu(II) is square planar and therefore an intermediate structure should require less energy in the redox process. Actually a recent X-ray crystal structure of plastocyanin [40] seems to confirm a distorted tetrahedral coordination, with bond angles deviating by as much as 50° from the values for a tetrahedon. From table 1 it appears that the largest coupling constants in CuX_4 chromophores are related to the bending vibrations $\epsilon(T_d$ symmetry) or $\beta_1(D_{2d}$ symmetry), which both tend to distort the chromophore towards a square planar form; in fact, since e_σ is always greater than e_π (as a rule, $e_\pi \sim 0.1$–$0.3\ e_\sigma$ [41]), the coupling constant is positive which implies a flattening of the tetrahedron [38].

As for the magnitude of e_λ and $(\partial e_\lambda/\partial R)$, their value can be evaluated theoretically, for example by the expressions (5) and (6), or deduced from the experimental data [15,38]; in general the larger values of e_λ are found in the higher oxidation states [7]; moreover e_π is not too different from zero in ammonia and aliphatic amines, while its contribution may be appreciable in aromatic or more "soft" ligands [41]. As for the sign of the parameters, e_σ corresponds to the energy increase of the d orbitals becoming σ-antibonding by combination with ligand σ orbitals and therefore it should be always positive; on the contrary ligands, which are π-acceptors towards the metal ion, have negative e_π, while positive e_π are characteristic of π-donors.

Besides copper (II), which is a well known Jahn-Teller ion, a strong JTE should be observed in low-spin cobalt(II) chromophores in octahedral (or nearly-octahedral) and trigonal bipyramidal (D_{3h}) coordination so that vibronic coupling has to be taken into account in considering the spectral and structural properties of the vitamin B_{12r}.

Apart from vitamin B_{12r}, few biologically interesting compounds have low-spin cobalt (II), whereas high-spin cobalt (II) commonly occurs when it substitutes

Table 1
Jahn-Teller coupling constants for transition metal ions commonly involved in metalloproteins

Electronic configuration	Ion	Point group	Electronic level a)	JT active vibrational mode b)	JT coupling matrix elements c)
d^1	Mo^{5+}	C_{4v}	$^2E(\xi,\eta)$	$\nu(\beta_1)$	$\langle\xi\vert\partial V/\partial S_{\beta_1}\vert\xi\rangle = -\frac{3}{4}\sin^2 2\theta\cdot\partial e_\sigma/\partial R + (\cos^2\theta - \cos^2 2\theta)\cdot\partial e_\pi/\partial R$
				$\delta(\beta_1)$	$\langle\xi\vert\partial V/\partial S_{\beta_1}\vert\xi\rangle = -(1/R)[\frac{3}{2}\sin 4\theta\cdot e_\sigma + (\sin 2\theta - 2\sin 4\theta)\cdot e_\pi]$
				$\delta(\beta_2)$	$\langle\xi\vert\partial V/\partial S_{\beta_2}\vert\eta\rangle = (2/R)(\cos^2 2\theta - \cos^2\theta)\cdot e_\pi$
		C_{3v}	$^2E(\xi,\eta)$	$\nu(\epsilon)$	$\langle\xi\vert\partial V/\partial S^{\epsilon}_{\zeta}\vert\xi\rangle = -\frac{1}{2}\sqrt{\frac{3}{2}}[\frac{3}{4}\sin^2 2\theta\cdot\partial e_\sigma/\partial R - (\cos^2\theta - \cos^2 2\theta)\cdot\partial e_\pi/$
				$\delta(\epsilon)$ d)	$\langle\xi\vert\partial V/\partial S^{\epsilon}_{\zeta}\vert\xi\rangle = (1/R)\sqrt{\frac{3}{2}}[-\frac{3}{4}\sin 4\theta\cdot e_\sigma + (-\frac{1}{2}\sin 2\theta + \sin 4\theta)\cdot e_\pi]$
				$\delta(\epsilon)$ e)	$\langle\xi\vert\partial V/\partial S^{\epsilon}_{\zeta}\vert\xi\rangle = -(1/R)\sqrt{\frac{3}{2}}[\frac{3}{4}\sin^2 2\theta\cdot e_\sigma + (\cos^2 2\theta - \cos^2\theta)\cdot e_\pi]$
d^5	Fe^{3+}	C_{4v}	$^2E(\xi^+\eta^2\zeta^2, \xi^2\eta^+\zeta^2)$	$\nu(\beta_1)$	$\langle\xi\vert\partial V/\partial S_{\beta_1}\vert\xi\rangle = \frac{3}{4}\sin^2 2\theta\cdot\partial e_\sigma/\partial R - (\cos^2\theta - \cos^2 2\theta)\cdot\partial e_\pi/\partial R$
				$\delta(\beta_1)$	$\langle\xi\vert\partial V/\partial S_{\beta_1}\vert\xi\rangle = (1/R)[\frac{3}{2}\sin 4\theta\cdot e_\sigma + (\sin 2\theta - 2\sin 4\theta)\cdot e_\pi]$
				$\delta(\beta_2)$	$\langle\xi\vert\partial V/\partial S_{\beta_2}\vert\eta\rangle = -(2/R)(\cos^2 2\theta - \cos^2\theta)e_\pi$
d^6	Fe^{2+} Co^{3+}	C_{4v}	$^5E(\xi^2\eta^+\zeta^+\epsilon^+\theta^+, -\xi^+\eta^2\zeta^+\epsilon^+\theta^+)$	$\nu(\beta_1)$	$\langle\xi\vert\partial V/\partial S_{\beta_1}\vert\xi\rangle = -\frac{3}{4}\sin^2 2\theta\cdot\partial e_\sigma/\partial R + (\cos^2\theta - \cos^2 2\theta)\cdot\partial e_\pi/\partial R$
				$\delta(\beta_1)$	$\langle\xi\vert\partial V/\partial S_{\beta_1}\vert\xi\rangle = -(1/R)[\frac{3}{2}\sin 4\theta\cdot e_\sigma + (\sin 2\theta - 2\sin 4\theta)\cdot e_\pi]$
				$\delta(\beta_2)$	$\langle\xi\vert\partial V/\partial S_{\beta_2}\vert\eta\rangle = (2/R)(\cos^2 2\theta - \cos^2\theta)\cdot e_\pi$
		T_d	$^5E(\epsilon^2\theta^+\xi^+\eta^+\zeta^+, \epsilon^+\theta^2\xi^+\eta^+\zeta^+)$	$\delta(\epsilon)$	$\langle\theta\vert\partial V/\partial S^{\epsilon}_{\theta}\vert\theta\rangle = -(4\sqrt{2}/3R)\cdot e_\pi$
d^7	Co^{2+}	O_h	$^2E_g(\xi^2\eta^2\zeta^2\theta^+, \xi^2\eta^2\zeta^2\epsilon^+$	$\nu(\epsilon)$	$\langle\theta\vert\partial V/\partial S^{\epsilon}_{\theta}\vert\theta\rangle = \frac{1}{2}\sqrt{3}\,\partial e_\sigma/\partial R$
		D_{3h}	$^2E'(\xi^2\eta^2\zeta^2\epsilon^+, \xi^2\eta^2\zeta^+\epsilon^2)$	$\nu(\epsilon')$	$\langle\epsilon\vert\partial V/\partial S^{\epsilon'}_{\zeta}\vert\epsilon\rangle = -\frac{1}{2}\sqrt{\frac{3}{2}}(\frac{3}{4}\partial e_\sigma/\partial R - \partial e_\pi/\partial R)$
				$\delta(\epsilon')$ f)	$\langle\epsilon\vert\partial V/\partial S^{\epsilon'}_{\zeta}\vert\epsilon\rangle = (1/R)\sqrt{\frac{3}{2}}(\frac{3}{2}e_\sigma - 2e_\pi)$
		C_{4v}	$^4E(\theta^+\epsilon^+\xi^+\eta^2\zeta^2, \theta^+\epsilon^+\xi^2\eta^+\zeta^2)$	$\nu(\beta_1)$	$\langle\xi\vert\partial V/\partial S_{\beta_1}\vert\xi\rangle = \frac{3}{4}\sin^2 2\theta\cdot\partial e_\sigma/\partial R - (\cos^2\theta - \cos^2 2\theta)\cdot\partial e_\pi/\partial R$
				$\delta(\beta_1)$	$\langle\xi\vert\partial V/\partial S_{\beta_1}\vert\xi\rangle = (1/R)[\frac{3}{4}\sin 4\theta\cdot e_\sigma + (\sin 2\theta - 2\sin 4\theta)\cdot e_\pi]$
				$\delta(\beta_2)$	$\langle\xi\vert\partial V/\partial S_{\beta_2}\vert\eta\rangle = -(2/R)(\cos^2 2\theta - \cos^2\theta)e_\pi$
d^9	Cu^{2+}	T_d	$^2T_2(\theta^2\epsilon^2\xi^+\eta^2\zeta^2, \theta^2\epsilon^2\xi^2\eta^+\zeta^2, \theta^2\epsilon^2\xi^2\eta^2\zeta^+)$	$\delta(\epsilon)$	$\langle\xi\vert\partial V/\partial S^{\epsilon}_{\epsilon}\vert\xi\rangle = (2\sqrt{6}/3R)(e_\sigma - \frac{1}{3}e_\pi)$
				$\nu(\tau_2)$	$\langle\xi\vert\partial V/\partial S^{\tau_2}_{\zeta}\vert\eta\rangle = -\frac{2}{3}(\partial e_\sigma/\partial R - \frac{1}{3}\partial e_\pi/\partial R)$
				$\delta(\tau_2)$	$\langle\xi\vert\partial V/\partial S^{\tau_2}_{\zeta}\vert\eta\rangle = (2\sqrt{2}/3R)(e_\sigma - \frac{7}{3}e_\pi)$
		D_{2d} g)	$^2E(\theta^2\epsilon^2\xi^+\eta^2\zeta^2, \theta^2\epsilon^2\xi^2\eta^+\zeta^2)$	$\delta(\beta_1)$	$\langle\xi\vert\partial V/\partial S_{\beta_1}\vert\xi\rangle = (\sqrt{6}/R)[\frac{3}{4}\sin^2 2\theta\cdot e_\sigma + (\cos^2 2\theta - \cos^2\theta)\cdot e_\pi]$
				$\nu(\beta_2)$	$\langle\xi\vert\partial V/\partial S_{\beta_2}\vert\eta\rangle = -\frac{3}{4}\sin^2 2\theta\cdot\partial e_\sigma/\partial R - 2(\cos^2 2\theta - \cos^2\theta)\cdot\partial e_\pi/\partial R$
				$\delta(\beta_2)$	$\langle\xi\vert\partial V/\partial S_{\beta_2}\vert\eta\rangle = -(2/R)[\frac{3}{4}\sin 4\theta\cdot e_\sigma - \frac{1}{2}(2\sin 4\theta - \sin 2\theta)\cdot e_\pi]$

a) Strong field configuration in parenthesis; $\xi, \eta, \zeta, \theta, \epsilon$ stand for the one-electron levels $d_{yz}, d_{xz}, d_{xy}, d_{z^2}$ and $d_{x^2-y^2}$ respectively.

b) The notation ν and δ refer to the stretching and bending vibrational modes, respectively.

c) Only one matrix element is reported for each case, since the other elements are easily obtained by symmetry considerations [15,38]; the angle θ corresponds to the angle between the main symmetry axis and the equatorial ligands; contributions from δ-bonds are neglected.

d) Out-of-plane bending. e) In-plane bending.

f) In-plane bending; in D_{3h} symmetry the coupling constants relative to the out-of-plane bending are zero.

g) In this case the angle θ corresponds to the angle between the S_4 symmetry axis and the M-X bond, where X is the ligand involved in the vibrational mode.

zinc (II) in zinc-containing metalloenzymes. In this latter case the ground electronic state is a non-degenerate level in tetrahedral ($^4A_2$) or pseudo-tetrahedral stereochemistry, which is the most likely geometry for cobalt (II) substituted zinc-enzymes [42], and therefore the JTE is absent. However, strong interactions are expected on the excited states and have to be considered, when an interpretation of the d-d absorption spectra is attempted.

With regard to other metal ions, we note that Mo(V), low-spin Fe(III) and high-spin Fe(II) should be affected, in the low-lying levels, by an appreciable JTE, particularly for five-coordinated chromophores, where the metal is situated out of the equatorial plane: such a situation for example is verified in deoxygenated homoproteins.

5. Application to deoxygenated hemoglobin and myoglobin

The magnetic susceptibility and Mössbauer data of DeoxyHb and DeoxyMb were simultaneously fitted for axial symmetry by considering vibronic coupling in the low-lying electronic levels [19]. Both molecules have, in C_{4v} symmetry, the following level scheme: $^5B_2 < {}^5E \sim {}^1A_1 < {}^3E$, in order of increasing energy; the first three levels are located within a few hundred cm^{-1} and the dynamical JTE on the state ^5E introduces a strong mixing and substantially modifies the level scheme, whereas the JTE on the level ^3E, owing to the larger separation ($\sim$2000 cm^{-1}) from the ground state, seems to be only a small perturbation. Given the mathematical complexity of the problem, various approximations were introduced and, in particular, only one out of three Jahn-Teller active vibrations ($2\beta_1 + \beta_2$) was considered, a vibration of β_1 symmetry. The resulting fit gave vibrational quanta of 50 and 57 cm^{-1} for DeoxyHb and DeoxyMb, respectively; these low values should very likely correspond to the out-of-plane bending of the square-pyramidal chromophore FeN_5.

The possibility of an easy evaluation of the Jahn-Teller coupling constants offered by the AOM, induced us to verify the validity of the above assumptions and to estimate the magnitude of the effect.

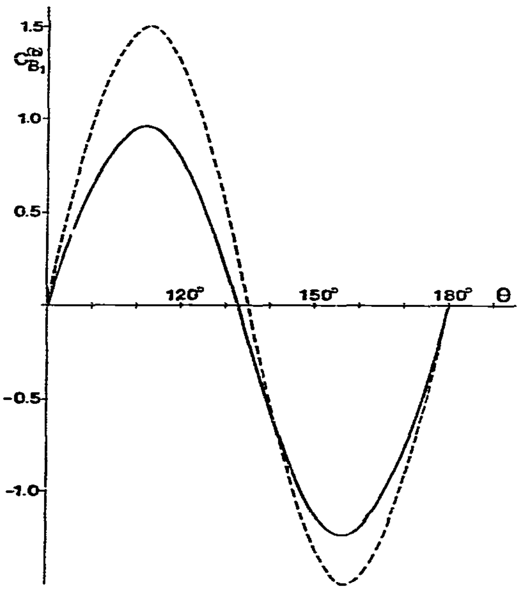

Fig. 1. Angular dependence of the Jahn-Teller coupling constant between the electronic state ^5E and the bending out-of-plane β_1, $C^{(b)}_{B_1} = \langle\eta|\partial V/\partial S_{\beta_1}|\eta\rangle$, for the Fe^{2+} ion in a square-pyramidal stereochemistry (C_{4v} symmetry). In ordinate the units are e_σ/R; $e_\pi = 0.2\ e_\sigma$ (solid line), $e_\pi = 0$ (dashed line).

Therefore, let us consider the level ^5E, arising from the octahedral term $^5T_{2g}$; if the mixing with the terms at higher energy is neglected, the expressions given in table 1 for Fe^{2+} in C_{4v} symmetry can be directly used.

In fig. 1 the coupling constant with the bending mode β_1 ($c^{(b)}_{B_1} = -\langle\xi|\partial V/\partial S_{\beta_1}|\xi\rangle$) is reported as function of the bond angle θ and two extreme values at 112.5° and 157.5° are found. If the last value is discarded as very unlikely, because it requires a too large displacement of the iron from the heme plane, we note that the value of 112.5° favourably compares with the experimental one of about 107° for DeoxyHb [32]. In the case of DeoxyMb the lower value of θ (about 98° [33]) still allows an appreciable coupling constant, owing to the steep slope of the curve (fig. 1). In other words one can say that such a geometry leads to a further energetic stabilization due to the JTE. Other factors which contribute in displacing the metal ion out of the heme plane are the too large size of the high-spin ferrous ion [43] and the energy level scheme for one-electron orbitals. In fact, as it appears from fig. 2, there is a *quasi*degeneracy of the ξ, η, ζ orbitals in

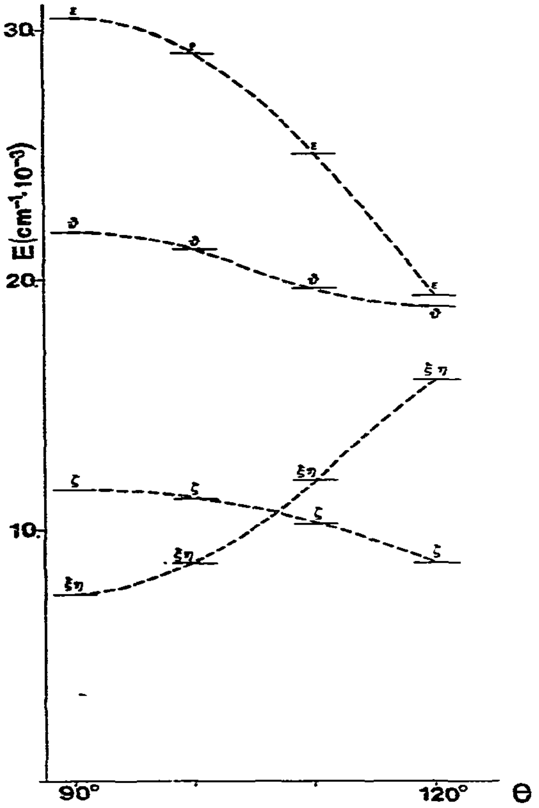

Fig. 2. Angular dependence of the one-electron orbital energies in a square-pyramidal stereochemistry (C_{4v} symmetry). The ligand field parameters are those of the fitting for DeoxyHb (see table 3).

the range 100–110° so that the high-spin configuration will be chiefly stabilized for these bond angles.

Using the X-ray data [32,33] and the expressions of table 1 we get the three Jahn-Teller constants for both molecules as function of e_λ and $(\partial e_\lambda/\partial R)$, as displayed in table 2. Since e_π is a fraction of e_σ, it is clear that the bending mode β_1 is more effective than the β_2 for vibronic coupling; more difficult is the comparison between the two β_1 modes.

We attempt now to perform a semi-quantitative evaluation of the constants and stabilization energies on the basis of the fits given in ref. [19], where the energy values of the one-electron d-orbitals were obtained from the relative energies of the many-electron low-lying levels $^1A_1$, ^3E, $^5B_2$ and ^5E [30]. Taking into account the geometry of the five-coordinated chromophore in DeoxyHb [32], it is a simple matter to derive from eq. (7) the energy values of the one-electron d-orbitals as a function of the AOM parameters:

$$e_\pi(N_{\mathrm{His}}^{\mathrm{Hb}}) + 0.470\, e_\sigma(N_{\mathrm{Pyr}}^{\mathrm{Hb}}) - 2.112\, e_\pi(N_{\mathrm{Pyr}}^{\mathrm{Hb}}) = 310\ \mathrm{cm}^{-1},$$

$$e_\sigma(N_{\mathrm{His}}^{\mathrm{Hb}}) + 0.553\, e_\sigma(N_{\mathrm{Pyr}}^{\mathrm{Hb}}) - 2.720\, e_\pi(N_{\mathrm{Pyr}}^{\mathrm{Hb}}) = 9527\ \mathrm{cm}^{-1}, \tag{9}$$

$$2.509\, e_\sigma(N_{\mathrm{Pyr}}^{\mathrm{Hb}}) - 3.345\, e_\pi(N_{\mathrm{Pyr}}^{\mathrm{Hb}}) = 15835\ \mathrm{cm}^{-1},$$

where $e_\lambda(N_{\mathrm{His}}^{\mathrm{Hb}})$ and $e_\lambda(N_{\mathrm{Pyr}}^{\mathrm{Hb}})$ stand for the λ-symmetry contributions ($\lambda = \sigma, \pi$) of the histidinic and pyrrolic nitrogen, respectively, in the DeoxyHb molecule. Analogously, for DeoxyMb we obtain:

$$e_\pi(N_{\mathrm{His}}^{\mathrm{Mb}}) + 0.128\, e_\sigma(N_{\mathrm{Pyr}}^{\mathrm{Mb}}) - 2.040\, e_\pi(N_{\mathrm{Pyr}}^{\mathrm{Mb}}) = 260\ \mathrm{cm}^{-1},$$

$$e_\sigma(N_{\mathrm{His}}^{\mathrm{Mb}}) + 0.873\, e_\sigma(N_{\mathrm{Pyr}}^{\mathrm{Mb}}) - 3.657\, e_\pi(N_{\mathrm{Pyr}}^{\mathrm{Mb}}) = 8837\ \mathrm{cm}^{-1}, \tag{10}$$

Table 2
Jahn-Teller coupling constants in the AOM for DeoxyHb and DeoxyMb [a)]

	DeoxyHb	DeoxyMb
$\langle\xi\vert\partial V/\partial S_{\beta_1}^{(s)}\vert\xi\rangle$	$-0.235\, \partial e_\sigma(N_{\mathrm{Pyr}}^{\mathrm{Hb}})/\partial R - 0.602\, \partial e_\pi(N_{\mathrm{Pyr}}^{\mathrm{Hb}})/\partial R$	$-0.064\, \partial e_\sigma(N_{\mathrm{Pyr}}^{\mathrm{Mb}})/\partial R - 0.893\, \partial e_\pi(N_{\mathrm{Pyr}}^{\mathrm{Mb}})/\partial R$
$\langle\xi\vert\partial V/\partial S_{\beta_1}^{(b)}\vert\xi\rangle$	$-0.662\, e_\sigma(N_{\mathrm{Pyr}}^{\mathrm{Hb}}) + 1.149\, e_\pi(N_{\mathrm{Pyr}}^{\mathrm{Hb}})$	$-0.411\, e_\sigma(N_{\mathrm{Pyr}}^{\mathrm{Mb}}) + 0.691\, e_\pi(N_{\mathrm{Pyr}}^{\mathrm{Mb}})$
$\langle\xi\vert\partial V/\partial S_{\beta_2}\vert\eta\rangle$	$0.573\, e_\pi(N_{\mathrm{Pyr}}^{\mathrm{Hb}})$	$0.874\, e_\pi(N_{\mathrm{Pyr}}^{\mathrm{Mb}})$

a) The labels (s) and (b) stand for stretching and bending, respectively; $N_{\mathrm{Pyr}}^{\mathrm{Hb}}$ and $N_{\mathrm{Pyr}}^{\mathrm{Mb}}$ indicate the pyrrolic nitrogen of the heme, in DeoxyHb and DeoxyMb, respectively.

Table 3
Ligand field parameters in the AOM, Jahn-Teller coupling constants and stabilization energies for DeoxyHb and DeoxyMb [a)]

	DeoxyHb	DeoxyMb
$e_\sigma(\mathrm{N_{Pyr}})$	$10175\ \mathrm{cm}^{-1}$	$6540\ \mathrm{cm}^{-1}$
$e_\pi(\mathrm{N_{Pyr}})$	$2900\ \mathrm{cm}^{-1}$	$665\ \mathrm{cm}^{-1}$
$e_\pi(\mathrm{N_{Pyr}})/e_\sigma(\mathrm{N_{Pyr}})$	0.28	0.10
$e_\sigma(\mathrm{N_{His}})$	$11785\ \mathrm{cm}^{-1}$	$5560\ \mathrm{cm}^{-1}$
$e_\pi(\mathrm{N_{His}})$	$1650\ \mathrm{cm}^{-1}$	$780\ \mathrm{cm}^{-1}$
$e_\pi(\mathrm{N_{His}})/e_\sigma(\mathrm{N_{His}})$	0.14	0.14
$\langle\xi\vert\partial V/S^{(b)}_{\beta_1}\vert\xi\rangle$	$-3405\ \mathrm{cm}^{-1}$	$-2230\ \mathrm{cm}^{-1}/\mathrm{Å}$
$\langle\xi\vert\partial V/\partial S_{\beta_2}\vert\eta\rangle$	$1660\ \mathrm{cm}^{-1}/\mathrm{Å}$	$580\ \mathrm{cm}^{-1}/\mathrm{Å}$
$\langle\xi\vert\partial V/\partial S^{(s)}_{\beta_1}\vert\xi\rangle$	$17350\ \mathrm{cm}^{-1}/\mathrm{Å}$	$5070\ \mathrm{cm}^{-1}/\mathrm{Å}$
$E_{\mathrm{JT}}[\beta_1^{(b)}]$	$\sim 1160\ \mathrm{cm}^{-1}$	$\sim 500\ \mathrm{cm}^{-1}$
$E_{\mathrm{JT}}[\beta_1^{(s)}]$	$\sim 610\ \mathrm{cm}^{-1}$	$\sim 50\ \mathrm{cm}^{-1}$
$E_{\mathrm{JT}}[\beta_2]$	$\sim 275\ \mathrm{cm}^{-1}$	$\sim 30\ \mathrm{cm}^{-1}$

[a)] The labels have the same significance, as in table 2.

$$2.870\, e_\sigma(\mathrm{N^{Mb}_{Pyr}}) - 3.828\, e_\pi(\mathrm{N^{Mb}_{Pyr}}) = 16222\ \mathrm{cm}^{-1}.$$

As we have three equations and four unknowns, we need a further relationship. If eq. (5) is considered and K_σ is assumed equal to K_π, the ratio (e_π/e_σ) is given by:

$$e_\pi/e_\sigma \sim (S_\pi/S_\sigma)^2. \tag{11}$$

The diatomic overlap integrals S_λ have been calculated at a distance corresponding to the Fe-histidine bond length, using the Slater orbitals reported by Zerner and Gouterman [44] for iron and nitrogen. We have found for both DeoxyHb and DeoxyMb a ratio $e_\pi(\mathrm{N_{His}})/e_\sigma(\mathrm{N_{His}}) \sim 0.14$; in this way the eqs. (9) and (10) can be solved and the results are reported in table 3. Even though the values of table 3 are of a qualitative nature important conclusions may be drawn. For example, it appears that an appreciable difference of the ratio $e_\pi(\mathrm{N_{Pyr}})/e_\sigma(\mathrm{N_{Pyr}})$ occurs for the two molecules, thus probably indicating a less "domed" structure of the heme ring in DeoxyMb.

As for the Jahn-Teller stabilization energy E_{JT}, given by

$$E_{\mathrm{JT}} = c^2/2K, \tag{12}$$

where c is the generic coupling constant, there is the problem of a very approximate knowledge of the force constant K. We have tentatively chosen 4.80 and 0.10 mdyne/Å for the stretching and the two bending modes, respectively, which correspond to frequencies of 350 cm^{-1} [45] and 50 cm^{-1} [19], if the effective mass of the pyrrole is used. For both molecules the prevalent stabilization is due to the bending β_1, thus confirming the validity of the approximation previously made [19], even if a strong difference with the fitting value ($E_{\mathrm{JT}} \sim 30\ \mathrm{cm}^{-1}$) is found. At this point some considerations are necessary. The three values of E_{JT} are probably affected by error to the same extent, because the same procedure was followed in their evaluation, so that the order of importance for the three distortions should be correct. Indeed the values of E_{JT} for the bending obtained in the present calculation appear too high, since a static JTE is unlikely for such systems, but an under-estimation of the force constants could partially account for this strong effect. On the other hand, an accurate treatment would require a dynamical description in which the different distorting modes are simultaneously considered.

6. Concluding remarks

In conclusion I want to stress that the JTE cannot be undervalued *a priori*, even if, as shown in the previous example of DeoxyHb and DeoxyMb, it is a not simple matter, for complicated systems as the biological ones to evaluate the different aspects of the problem, which requires, together with the theoretical elaboration, a deeper experimental work.

References

[1] See for example:
B.L. Vallee and W.E.C. Wacker, The Proteins, Vol. V, Metalloproteins, ed. H. Neurath (Academic Press, New York, 1970);
M.N. Hughes, The inorganic chemistry of biological processes (Wiley-Interscience, New York, 1972);
A.S. Brill, Transition metals in biochemistry (Springer, Berlin, 1977).
[2] B.L. Vallee and R.J.P. Williams, Proc. Natl. Acad. Sci. (U.S.) 59 (1968) 498.
[3] M. Weissbluth, Hemoglobin (Springer, Berlin, 1974).
[4] C.K. Jørgensen, R. Pappalardo and H.H. Schmidtke, J. Chem. Phys. 39 (1963) 1422.
[5] C.E. Schäffer and C.K. Jørgensen, Mol. Phys. 9 (1965) 401.

[6] C.E. Schäffer, Structure and bonding 5 (1968) 68.
[7] C.K. Jørgensen, Modern aspects of ligand field theory (North Holland, Amsterdam, 1971).
[8] W. DeW. Harrocks, Jr. and D.A. Burlone, J. Am. Chem. Soc. 98 (1976) 6512.
[9] M. Wolfsberg and L. Helmholz, J. Chem. Phys. 20 (1952) 837.
[10] H.A. Jahn and E. Teller, Proc. Roy. Soc. A 161 (1937) 220.
[11] R. Englman, The Jahn-Teller effect in molecules and crystals (Wiley, New York, 1972).
[12] J.H. Van Vleck, J. Chem. Phys. 7 (1939) 72.
[13] A.D. Liehr and C.J. Ballhausen, Ann. Phys. (N.Y.) 3 (1958) 304.
[14] C.J. Ballhausen and J. de Heer, J. Chem. Phys. 43 (1965) 4304.
[15] M. Bacci, Chem. Phys. Letters 58 (1978) 537.
[16] I.B. Bersuker, Coord. Chem. Rev. 14 (1975) 357.
[17] H. Kamimura and S. Mizuhashi, J. Appl. Phys. 39 (1968) 684.
[18] S. Mizuhashi, J. Phys. Soc. Jpn. 26 (1969) 468.
[19] M. Bacci, J. Chem. Phys. 68 (1978) 4907.
[20] M. Weissbluth, J. Theor. Biol. 35 (1972) 597.
[21] M. Weissbluth, in: Computational methods for large molecules and localized states in solids, eds. F. Herman, A.D. McLean and R.K. Nesbet (Plenum Press, New York, 1973) p. 59.
[22] L. Cianchi, F. Gulisano, M. Mancini and G. Spina, Phys. Letters 59A (1976) 247.
[23] I.Y. Chan, W.G. van Dorp, T.J. Schaafsma and J.H. van der Waals, Mol. Phys. 22 (1971) 741, 753; M. Gouterman, Ann. N.Y. Acad. Sci. 206 (1973) 70.
[24] G.W. Canters, G. Jansen, M. Noort and J.H. van der Waals, J. Phys. Chem. 80 (1976) 2253.
[25] E.C.M. Kielman-Van Luijt, H.P.J.M. Dekkers and G.W. Canters, Mol. Phys. 32 (1976) 899.
[26] J.A. Shelnutt, L.D. Cheung, R.C.C. Chang, Nai-Teng Yu and R.N. Felton, J. Chem. Phys. 66 (1977) 3387.
[27] H. Eicher and A. Trautwein, J. Chem. Phys. 50 (1969) 2540.
[28] B.N. Huynh, G.C. Papaefthymiou, C.S. Yen, J.L. Groves and C.S. Wu, J. Chem. Phys. 61 (1974) 3750.
[29] A. Trautwein, R. Zimmermann and F.E. Harris, Theor. Chim. Acta Berlin 37 (1975) 89.
[30] H. Eicher, D. Bade and F. Parak, J. Chem. Phys. 64 (1976) 1446.
[31] D. Bade and F. Parak, Biophys. Struct. Mech. 2 (1976) 219.
[32] M.F. Perutz, Nature 228 (1970) 726;
G. Fermi, J. Mol. Biol. 97 (1975) 237.
[33] C.L. Nobbs, H.C. Watson and J.C. Kendrew, Nature 209 (1966) 339.
[34] J.C.W. Chien and L.C. Dickinson, Proc. Nat. Acad. Sci. USA 69 (1972) 2783;
L.C. Dickinson and J.C.W. Chien, Biochem. Biophys. Res. Commun. 51 (1973) 587;
T. Yonetani, H. Yamamoto and T. Iizuka, J. Biol. Chem. 249 (1974) 2168.
[35] M. Bacci, Chem. Phys. Letters 48 (1977) 184.
[36] Y. Alpert and R. Banerjee, Biochim. Biophys. Acta 405 (1975) 144.
[37] S. Califano, Vibrational states (Wiley, New York, 1976).
[38] M. Bacci, Chem. Phys., 40 (1979) 237.
[39] A.J. Fee, Structure and Bonding 23 (1975) 1.
[40] P.M. Colman, H.C. Freeman, J.M. Guss, M. Murata, V.A. Norris, J.A.M. Ramshaw and M.P. Venkatappa, Nature 272 (1978) 319.
[41] D.W. Smith, Structure and Bonding 35 (1978) 87.
[42] S. Lindskog, Structure and Bonding 8 (1970) 153.
[43] J.T. Hoard, Science 174 (1971) 1295.
[44] M. Zerner and M. Gouterman, Theor. Chim. Acta 4 (1966) 44.
[45] H. Brunner and H. Sussner, Biochim. Biophys. Acta 310 (1973) 20.